Research, Society and Development, v. 11, n. 5, e34511528144, 2022
(CC BY 4.0) | ISSN 2525-3409 | DOI: http://dx.doi.org/10.33448/rsd-v11i5.28144

Mechanical behaviour of femur and humerus at the three-point bending and axial compression tests in the crab-eating fox (*Cerdocyon thous*, Linnaeus 1776)

Biomecânica do fêmur e úmero de cachorros-do-mato (*Cerdocyon thous*, Linnaeus 1776) aos ensaios de flexão em três pontos e compressão axial

Biomecánica del fémur y húmero del zorro cangrejero (Cerdocyon thous, Linnaeus 1776) en ensayos de flexión de tres puntos y compresión axial

Received: 03/16/2022 | Reviewed: 03/24/2022 | Accept: 04/02/2022 | Published: 04/09/2022

Felipe Martins Pastor
ORCID: https://orcid.org/0000-0001-9447-5055
Universidade Federal do Espírito Santo, Brazil
E-mail: felipempastor@gmail.com
Gabriela de Oliveira Resende
ORCID: https://orcid.org/0000-0001-7444-5342
Universidade Federal do Espírito Santo, Brazil
E-mail: gabrielaoresende@hotmail.com
Rejane Costa Alves
ORCID: https://orcid.org/0000-0003-4059-3974
Universidade Federal do Espírito Santo, Brazil
E-mail: rejanealves.ufes@gmail.com
Louisiane de Carvalho Nunes
ORCID: https://orcid.org/0000-0003-4924-0614
Universidade Federal do Espírito Santo, Brazil
E-mail: louisianecn@gmail.com
Guilherme Galhardo Franco
ORCID: https://orcid.org/0000-0001-9945-3453
Universidade Federal do Espírito Santo, Brazil
E-mail: guilherme.franco.vet@gmail.com
Jankerle Neves Boeloni
ORCID: https://orcid.org/0000-0003-0049-6854
Universidade Federal do Espírito Santo, Brazil
E-mail: jankerle@gmail.com
Rogéria Serakides
ORCID: https://orcid.org/0000-0001-5374-6242
Universidade Federal de Minas Gerais, Brazil
E-mail: serakidesufmg@gmail.com
Maria Aparecida da Silva
ORCID: https://orcid.org/0000-0003-0967-3925
Universidade Federal do Espírito Santo, Brazil
E-mail: mvmariaaparecida@gmail.com

Abstract
The aim of the present study was to evaluate the mechanical behaviour of the femur and humerus of *Cerdocyon thous* through three-point bending and axial compression tests. For this, 13 femurs and 15 humerus were used in the bending test, and 14 femurs and 15 humerus in the compression test; after the assays were completed, bone fragments were collected for evaluation by means of conventional optical and polarized light microscopy, and scanning electron microscopy. It was observed that the humerus is more resistant in relation to the femur in both tests, and that bone length and weight, in addition to the width of the diaphysis, are influential on the mechanical behaviour. Microscopic evaluation showed that, on the cranial surface of the fractured bones under flexion, the fracture was caused by the deflection mechanism, while the caudal surface was ruptured by delamination. In bones submitted to axial compression, diaphyseal fractures occurred by deflection, while physeal fractures were caused by several mechanisms. There was no significant correlation between the arrangement of collagen fibres or mineral content on the mechanical properties obtained in both assays. It can be concluded that there are significant differences in the mechanical behaviour of the femur and humerus of *C. thous*, where the humerus is more resistant than the femur in both flexion and compression loads. Such data allow us to predict the bone mechanical behaviour of *C. thous* in the face of trauma caused by flexion and compression impacts, such as those resulting from running over.
Keywords: Bone biology; Fracture mechanics; Orthopaedics; Scanning electron microscopy.

Resumo

O presente estudo foi conduzido com objetivo de avaliar o comportamento mecânico do fêmur e úmero de *Cerdocyon thous* por meio dos ensaios de flexão em três pontos e compressão axial. Para tal, foram utilizados 13 fêmures e 15 úmeros no ensaio de flexão, e 14 fêmures e 15 úmeros no ensaio de compressão; finalizados os ensaios, foram coletados fragmentos ósseos para avaliação por meio de microscopia ótica convecional e de luz polarizada, e microscopia eletrônica de varredura. Observou-se que o úmero é mais resistente em relação ao fêmur em ambos os ensaios, e que comprimento e peso ósseos, além da largura da diáfise são influentes sobre o comportamento mecânico. A avaliação microscópica mostrou que, na face cranial dos ossos fraturados sob flexão, a fratura foi causada pelo mecanismo de deflexão, enquanto a face caudal se rompeu por delaminação. Nos ossos submetidos à compressão axial, as fraturas diafisárias ocorreram por deflexão, enquanto as fisárias foram originadas por diversos mecanismos. Não houve correlação significativa entre a disposição das fibras colágenas ou conteúdo mineral sobre as propriedades mecânicas obtidas em ambos os ensaios. Pode-se concluir que existem diferenças significativas no comportamento mecânico do fêmur e úmero de *C. thous*, onde o úmero é mais resistente que o fêmur tanto nas cargas de flexão quanto nas de compressão. Tais dados permitem prever o comportamento mecânico ósseo de *C. thous* frente a traumas causados por impactos de flexão e compressão, como aqueles resultantes de atropelmentos.

Palavras-chave: Biologia óssea; Mecânica da fraturas; Ortopedia; Microscopia eletrônica de varredura.

Resumen

El presente estudio se realizó con el objetivo de evaluar el comportamiento mecánico del fémur y húmero de *Cerdocyon thous* mediante ensayos de flexión en tres puntos y compresión axial. Para ello se utilizaron 13 fémures y 15 húmeros en la prueba de flexión, y 14 fémures y 15 húmeros en la prueba de compresión; una vez finalizadas las pruebas, se recogieron fragmentos óseos para su evaluación mediante microscopía óptica convencional y de luz polarizada, y microscopía electrónica de barrido. Se observó que el húmero es más resistente en relación al fémur en ambas pruebas, y que la longitud y el peso del hueso, además del ancho de la diáfisis, influyen en el comportamiento mecánico. La evaluación microscópica mostró que, en la superficie craneal de los huesos fracturados bajo flexión, la fractura fue causada por el mecanismo de desviación, mientras que la superficie caudal se rompió por delaminación. En huesos sometidos a compresión axial, las fracturas diafisarias ocurrieron por deflexión, mientras que las fracturas fisarias fueron causadas por varios mecanismos. No hubo correlación significativa entre la disposición de las fibras de colágeno o el contenido de minerales sobre las propiedades mecánicas obtenidas en ambos ensayos. Se puede concluir que existen diferencias significativas en el comportamiento mecánico del fémur y húmero de *C. thous*, donde el húmero es más resistente que el fémur tanto en cargas de flexión como de compresión. Dichos datos nos permiten predecir el comportamiento mecánico óseo de *C. thous* ante traumatismos por impactos de flexión y compresión, como los resultantes del pisoteo.

Palabras clave: Biología ósea; Mecánica de fractura; Ortopedia; Microscopía electrónica de barrido.

1. Introduction

Cerdocyon thous (crab-eating fox) is one of the six species of the canid family native to South America. This species has the widest distribution compared with others. It is currently found in almost every country on the subcontinent, with the exception of parts of the Amazon, Ecuador, Peru, and Chile (Courtenay and Maffei 2004). Despite its wide geographic distribution, *C. thous* suffers from constant threats towards its preservation. Since the species cohabits anthropic environments, roadkill's and hunting are the main causes of mortality (Berta 1982; Ginsberg and Macdonald 1990).

According to Grilo et al. (2018), *C. thous* was the third wild species with the highest mortality among the 450 identified in the study that are victims of run-over accidents on Brazilian highways. Araújo Cezar et al. (2021) also confirmed the high mortality of *C. thous* on highways in northeastern Brazil, with this species accounting for 79.5% of the total number of dead animals. In the transition region of Amazonia and Cerrado, *C. thous* was also the most trampled species (Brum et al. 2018). However, the high rate of deaths due to being run over does not occur exclusively on the Brazilian highways, as *C. thous* was the second most frequently run-over mammalian species in Colombia (Ossa-Nadjar and Ossa 2013).

In addition to immediate death, one of the main consequences of being run over by motor vehicles includes bone fractures (Trapp et al. 2010), which represent the main orthopaedic conditions in wild canids (Carlton and Mcgavin 1998; Pessutti et al. 2001). To predict the mechanical behaviour of the tissue in the face of different types of impact and its implications on the genesis of fractures, biomechanical assessment of the bone is configured as a highly effective tool (Markel et al. 1994; Nishioka et al. 2010). In addition to predicting the aetiology of fractures, research on bone biomechanics aims to elucidate *in vivo* bone

behaviour considering the absorptive energy capacity of the organ, resistance to deformation, and muscle strains to which it is predisposed. The study of bone biomechanics may also clarify the way in which tissue architecture influences the mechanical properties (Currey 1970).

In addition, research aimed at the mechanical properties of bone tissue is relevant in the development of biomaterials used as tissue substitutes, whether in cases of fractures, bone loss due to necrosis, neoplasms, or joint diseases. It is crucial that the material used has mechanical properties, such as toughness and strength, similar to the bone so that its use is effective (Rho et al. 1998; Wang et al. 2002; Zadpoor 2015). Thus, biomechanical evaluation provides the necessary knowledge to understand the mechanical influences that act on bone tissue, and therefore, estimate the maximum load values and energy impact that these tissues are able to absorb until fractures occur. On this basis, it is possible to predict the types of fractures and their likely locations along the bone axis, as well as to characterise the degree of influence of certain properties on tissue strength.

Despite the morphological similarity of the skeletons of wild canids and domestic dogs, there are specific anatomical and functional characteristics. Thus, the data obtained from studies carried out in domestic dogs are not entirely applicable to *C. thous,* requiring in-depth evaluation of the species in question (Pinheiro et al 2015; Castilho et al 2018; Vélez et al 2018; Martins et al 2021).

Utilising the knowledge of bone biomechanics applied to the species, it is possible for clinicians and surgeons to adopt the most appropriate therapeutic approach in each case of trauma in wild canids. It is expected that, with the improvement in the treatment of bone fractures in these wild canids, the reinsertion of these individuals in their natural habitat will become sooner and more effective, thus contributing to the preservation of the species.

In view of this, the present research was conducted with the objective of comparing the existence of differences between the mechanical behaviour of the femur and humerus of *C. thous* under the three-point bending and axial compression tests, as well as evaluating the possible influence of morphometric and microstructural characteristics on bone resistance in such species.

2. Methodology

The guidelines of the National Council for the Control of Animal Experimentation (CONCEA) were followed. This study was conducted with the approval of the Council for Ethics in the Use of Animals of the Universidade Federal do Espírito Santo, under protocol No. 65/2017.

Animal selection

In the present study, the 18 cadavers of *Cerdocyon thous* used were obtained through donations made by the Reserva Biológica de Sooretama (ES) (n=11), Instituto Brasileiro do Meio Ambiente e dos Recursos Naturais Renováveis (IBAMA) (n=2), and the Hospital Veterinário da Universidade Federal do Espírito Santo, Brazil (n=5). All these animals were killed by being run over on the side of roads or died from complications related to trauma from being run over. In addition, all cadavers within 12 h of death were used.

Among the sample, 12 males (five youngsters and seven adults) and six females (three youngsters and three adults) were identified, weighing between 3.7 and 6.1 kg. Necroscopic examination was performed at the Animal Pathology Laboratory of the Universidade Federal do Espírito Santo. The thoracic and pelvic limbs along with femurs and humerus dissected. Among the bones, 13 left and 14 right femurs, and 15 left and 15 right humeri without macroscopic signs of bone or joint affections were selected.

In all bones, the weight, total length, and circumference of the diaphysis (obtained at the midpoint of the diaphysis, based on the total length) were measured. Subsequently, the bones were packed in plastic bags, identified, and frozen at -20 °C.

Three-point bending test

To perform the three-point bending test, 13 left femurs and 15 left humerus were used. The bones were transported in coolers to the Wood Science Laboratory, *Universidade Federal do Espírito Santo, Brazil*. The samples were maintained at room temperature (25 °C) for at least two h until complete defrosting.

The three-point bending tests were performed on an Emic DL10000 (São José dos Pinhais, PR, BR) universal testing machine, equipped with data acquisition software Tesc 3.04 (Intermetric, Mogi das Cruzes, SP, BR). The methodology used was based on the standard D790-17 of the American Society for Testing Materials (ASTM 2017), which standardizes the three-point bending tests for unreinforced and reinforced plastics.

The bones were positioned longitudinally, so that the load was applied in the central region of the diaphysis in a craniocaudal direction (Fig 1a). The distance between the supports was maintained as 5 cm using a 500 kgf load cell, with a speed of 1 mm/min and minimum deformation of the specimen was maintained as 70%. The load was applied until fracture occurred, and at the end of the test, the values of maximum load, strength, modulus of rupture, modulus of elasticity, and work were established.

Figure 1. Methodology used in the three-point bending and axial compression tests. (A) Positioning of the bone with the application of the load in the central region of the femoral diaphysis in the three-point bending test. (B) Positioning of the bone with the application of the load in the femoral proximal epiphysis in the axial compression test. (C) Scheme of bone sections sent for microscopic evaluation: energy-dispersive X-ray spectroscopy (EDS); scanning electron microscopy (SEM); decalcification and evaluation under optical microscopy (D-OM); grinding and evaluation under polarized light microscopy (G-PLM).

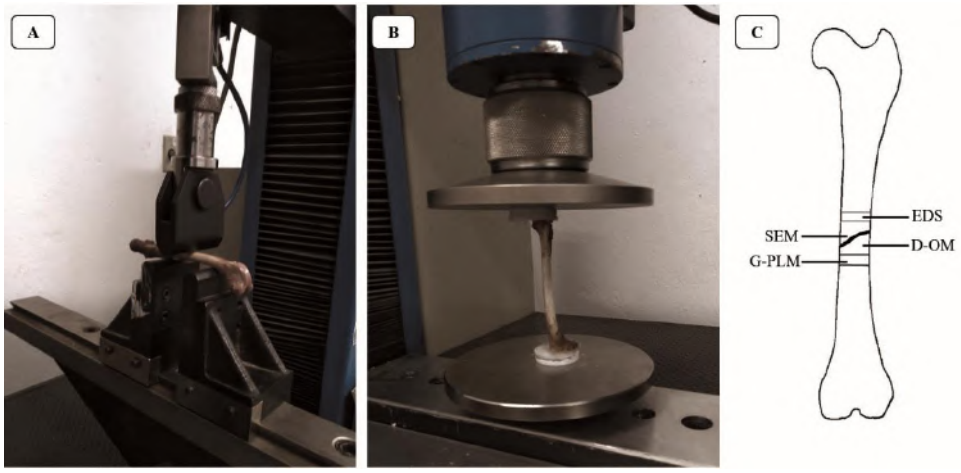

Source: The authors.

Axial compression test

In order to perform the axial compression test, 14 right femurs and 15 right humerus were used. After dissection, the tips of the epiphyses were embedded in epoxy resin blocks in order to maintain the positioning and prevent slippage of the specimen during testing. After the resin was completely dried, the bones were immediately stored at a temperature of -20 °C until the date of the test. The bones were then maintained at room temperature (25 °C) for at least two hours until complete defrosting.

The axial compression biomechanical tests were carried out in an Emic DL10000 universal testing machine (São José dos Pinhais, PR, BR), at the Wood Science Laboratory, *Universidade Federal do Espírito Santo, Brazil*. The methodology

followed the standards established by the technical standard NBR-7190 of the Brazilian Association of Technical Standards (ABNT 1997), which standardizes the mechanical tests on wooden structures.

The bones were positioned vertically, so that the load cell applied force to the proximal epiphysis, in the near-distal direction (Fig 1b). A 1000 Kgf load cell was used, with force applied at 1 mm/min, with a 70% deformation. The load was applied to the bone until the fracture occurred, and at the end of the test, the values of parallel compression, maximum force, and resistance were established.

Macroscopic classification of fractures

After the mechanical tests, the bones were cooled immediately and subsequently subjected to the classification of fractures, as proposed by Unger et al (1990) and Salter and Harris (1963). The authors group the injuries according to anatomical location, number of fragments, severity, and direction of the fracture line.

Microscopic analysis of fracture fragments

After the classification of the fractures, four bone sections approximately 1 cm high were made using a band saw (Fig 1c). The fragments proximal to the fracture line were washed in a phosphate-buffered saline solution (PBS, pH 7.2) to remove blood, bone marrow, and other soft tissues, and fixed in a 2.5% glutaraldehyde solution for 24 h. Subsequently, the fragments were processed according to the techniques of scanning electron microscopy (SEM) and energy-dispersive X-ray spectroscopy (EDS). For this, the samples were washed in distilled water and dehydrated in ethanol in increasing concentrations (30%-100%), being subsequently dried in an oven at 37 °C for a period of 24 h. Since the dehydration process was effective, it was decided not to carry out the critical point drying.

The SEM and EDS analyzes were performed at the Cell Ultrastructure Laboratory Carlos Alberto Redins (LUCCAR), from the Health Sciences Centre of the *Universidade Federal do Espírito Santo*. All the samples were metallized by gold evaporation (Denton Vacuum Desk V, Moorestown, NJ, USA), and then evalueted at a JEOL JSM-6610 (Akishima, TO, JP) scanning electron microscope equipped with an EDS ultra-thin polymer window. The samples were evaluated at 50×, 200× and 1200× magnifications, with the purpose to evaluate the fracture surface morphology and mechanism of tissue rupture. Through the EDS technique, the qualitative mineral distribution on the surface of the fracture fragments was obtained, as well as the quantitative values (g/mol) of the concentration of each of the chemical components.

The distal fragments of the fracture line were fixed in 10% formalin for at least 48 h. Then, the fragment containing the distal fracture surface was decalcified based on the protocol proposed by Morse (1945), with a solution of formic acid and sodium citrate. Subsequently, it was processed according to the histological technique for paraffin embedding and stained with haematoxylin and eosin. The cell morphology and tissue activity analyses were performed in a Leica ICC50 HD (Wetzlar, DE) optical microscope, in which the fragments were evaluated at 10× and 40× magnifications.

Meanwhile, the distal fragment was subjected to the preparation of histological slides by manual grinding technique, to the thickness of 100 μm, approximately. The fragments were then evaluated by polarized light microscopy in a Nikon E200 (Minato, TO, JP) optical microscope, from the Microscopy Laboratory of the Department of Geology, Unversidade Federal do Espírito Santo. The samples were observed at 10× and 40× magnification, being evaluated the spatial orientation of collagen type I fibres in osteons, according to the classification proposed by Ascenzi and Bonucci (1968). With the images obtained with 40× amplification, the area occupied by the transverse fibres was calculated using the software ImageJ (National Institutes of Health, Bethesda, MD, USA). The same slides were also used to obtain the mean thickness of the cortical bone layer under a Leica ICC50 HD (Wetzlar, DE) optical microscope. The fragments were photographed at four equidistant points, using the 40×

magnification, and then the measurements were performed using the LAS EZ 3.04 (Leica, Wetzlar, DE) software, obtaining the final average of the four measurements.

Statistical analysis

To verify the differences between the mechanical behaviour of bones under the tree-point bending test, the averages of the values obtained for the mechanical properties (maximum load, strength, modulus of rupture, modulus of elasticity, and work) were compared between the femur and humerus, and between males and females for each bone. For this purpose, the F test ($p < 0.05$) was used in addition to the Tukey test ($p < 0.05$), where significant differences were observed between the means of each property. Similarly, the mechanical behaviour of bones under the axial compression test was compared. For this, the values obtained (maximum load, parallel compression and strength) were compared between femur and humerus, and between males and females, using the F and Tukey tests ($p < 0.05$). In addition, the mechanical behaviour of the bones was compared between the three-point bending and axial compression tests, and the values of maximum load and resistance were compared using the F and Tukey tests ($p < 0.05$).

To assess the possible influence of the maximum load on the type of fracture generated in the mechanical tests, a simple linear regression test was performed ($p < 0.05$). To this end, numerical values were assigned to each type of fracture, and then, these values were compared to those of the maximum load.

To assess the degree of influence of morphometric (length, weight, diaphysis circumference, and bone cortical thickness) and microstructural characteristics (area occupied by transverse collagen fibres and mineral content) on the mechanical behaviour of bones, a simple linear regression test ($p < 0.05$) was used. The influence of such characteristics on the mechanical properties obtained in each mechanical test was verified by individually comparing each value. All statistical analyses were performed using the statistical software BioEstat 5.0 (Instituto Mamirauá, Tefé, AM, BR).

3. Results

Mechanical tests

The load-displacement curves associated with the mechanical tests on *Cerdocyon thous* femur and humerus are shown in Figure 2. When analysing them, it is noted that the bones have both ductile and fragile characteristics. The humerus, in both tests, showed a greater elastic deformation region and a less pronounced elastic limit. In the axial compression curves, we observed an initial growing region, followed by a small drop in the load value. This region represents the moment of adjustment of the resin blocks, which presented a slight displacement caused by the application of the initial load. It is still possible to observe the change in the slope of the curves during the tests, which occurred in the deformation interval of 2-3 mm (three-point bending test) and 4-5 mm (axial compression test). It is observed that the values of maximum strength as well as higher values of toughness, represented by the total area under the curve, were higher for the humerus when compared to femurs in both assays.

Figure 2. Load-displacement curves obtained in the three-point bending test (left femur and humerus) and axial compression test (right femur and humerus).

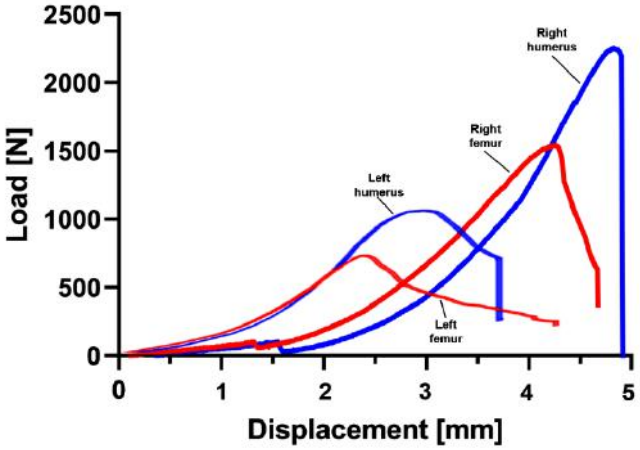

Source: The authors.

Table 1 shows the mean values of the mechanical properties determined during the mechanical tests. There were no statistically significant differences between the mechanical properties of males and females (data not shown); thus, data for both sexes were grouped. It may be seen that there was a significant difference in the maximum strength and resistance between the tested bones. This information allows us to conclude that the humerus needs a greater load for the fracture to occur when compared to the femur.

Table 1. Mean values of maximum load, strength, parallel compression, modulus of rupture (MOR), modulus of elasticity (MOE), and work obtained in the mechanical tests of femurs and humerus of *Cerdocyon thous*.

	THREE-POINT BENDING		**AXIAL COMPRESSION**	
	Humerus	**Femurs**	**Humerus**	**Femurs**
Maximum load [N]	718.95 A,b	450.68 B,b	1881.7 A,a	1300.95 B,a
Strength [MPa]	7.416 A,b	5.53 B,b	20.081 A,a	14.15 B,a
Parallel compression [MPa]	*	*	20.36 A	14.18 B
MOR [MPa]	58.88 A	57.29 A	*	*
MOE [MPa]	2898.30 A	3701.59 A	*	*
Work [J]	1.13 A	0.43 B	*	*

Mean values followed by different uppercase letters indicate a statistically significant difference between the characteristics obtained in the same type of test ($p < 0.05$). Mean values followed by different lowercase letters indicate a significant difference between the characteristics when compared between the two tests. ($p < 0.05$). *: Values not established in the test. Source: The authors.

The results obtained for the linear regression for the femur showed that the circumference of the diaphysis has a low influence on the modulus of elasticity (R2 = 31.83%) (Figure 3a). Likewise, the diaphysis circumference could influence the modulus of elasticity of the humerus (R2 = 64.93%) (Figure 3b). Meanwhile, the maximum strength was influenced by variations

in the length (R2 = 55.24%) and bone weight (R2 = 67.92%) of the humerus (Figure 3c and 3d) in the bending test, and by the diaphysis circumference in compression (R2 = 30.54%) (Figure 3e).

Figure 3. Graphs of significant linear regression (p <0.05) for morphometric characteristics and the mechanical properties of *Cerdocyon thous* femurs and humerus. (A) Femur in the three-point bending test. (B, C, and D) Humerus in the three-point bending test. (E) Humerus in the axial compression test.

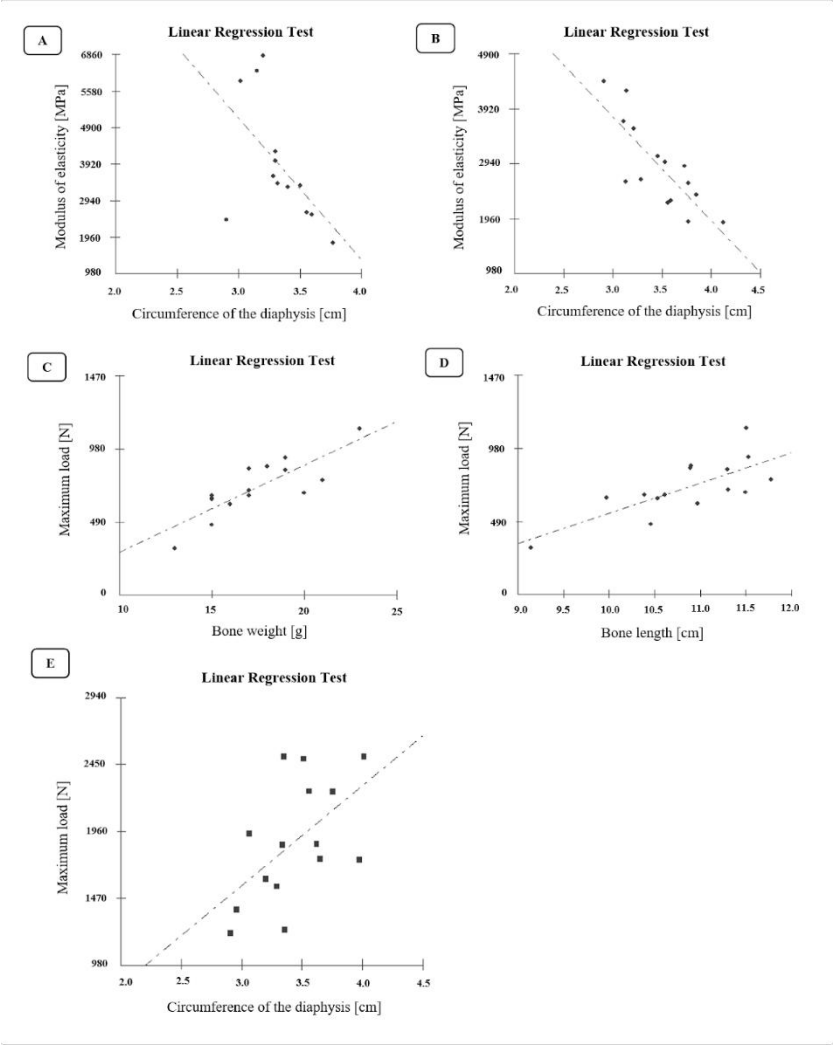

Source: The authors.

Macroscopic classification of fractures

According to the macroscopic classification, all fractures caused by the three-point bending test in femurs and humerus occurred in the diaphysis, because of load application during the test. One of the fractures in the femur was fragmented wedge type (B3) (7.69%). The others (92.32%) varied in equivalent proportions between simple transverse (A3) and oblique (A2). In the humerus, simple oblique fractures (A2) were the most prevalent (66.67%) in relation to the transversal fractures (A3) (33.33%).

Meanwhile, in the axial compression test, fractures showed great variation in the number of fragments, severity and in the direction of the fracture line. In the femur, 35.71% of the fractures were simple (oblique, 40%; transverse, 60%), and 57.14% were complex (type C) (segmented (C2), 50%; comminuted (C3), 50%). In addition, a type II Salter-Harris fracture was also observed in the distal epiphysis (7.14%). In turn, in the humerus, 46.67% of the fractures were simple (oblique, 71.43%;

transverse, 28.57%), while 40% were complex (segmented, 66.67%; comminuted, 33.33%). Type I (6.67%) and type II (6.67%) Salter-Harris fractures were also observed in the proximal and distal epiphyses, respectively. No significant results were found for the correlation between the type of fracture and the maximum load or the bone strength

Microscopic analysis of fracture fragments

During the assessment of tissue morphology and cell activity, secondary bone tissue was observed to be morphologically viable and well organized in the form of osteons and circumferential lamellae, in all samples of diaphyseal fractures (Figure 4a). In the case of the physeal fractures (Fig 4b), there was a predominance of primary bone tissue, formed from by thick and confluent trabeculae.

During the evaluation of the orientation of type I collagen fibres by polarized light microscopy in diaphyseal fractures (Figure 4c), the presence of all three types of osteons was verified, with two (intermediate) and three (dark) being predominant. In all fractures originating in the bone epiphyses, the collagen fibres were arranged without apparent pattern, oriented in both transversal and longitudinal direction (Figure 4d). There was no significance for linear regression between the area occupied by the transversal collagen fibres and the mechanical properties obtained in the three-point bending test.

Morphological evaluation of the fracture surface and mechanism of tissue rupture by scanning electron microscopy revealed differences between the bones evaluated in bending and compression tests. In the three-point bending samples, there were two distinct patterns, which were repeated in the femur and humerus. On the cranial bony face, where there was load application and greater compression action, the surface was predominantly smooth, with few microcracks and osteons with few distinct lamellae, suggesting a deflection mechanism (Figure 5a and 5b). On the caudal face of the diaphysis where the traction load became more evident, the surface was rough, and the microcracks were arranged around the osteons, which have a delamination characteristic (Figure 5c and 5d). It was observed that 64% of the transverse fractures in femur and humerus had a mechanism of rupture by delamination more evident than the deflection. However, only 25% of oblique fractures in all bones showed a more pronounced delamination pattern than deflection.

Figure 4. Microscopic evaluations of the fracture region in the femur and humerus of *Cerdocyon thous* submitted to the mechanical tests. (A) Photomicrograph of a fragment of femur showing secondary bone tissue composed of interstitial lamellae and osteons, with osteocytes inside the gaps (arrow). Bar: 100 µm. (B) Primary bone tissue in a fracture fragment in the femur epiphysis, composed of thick trabeculae (arrow). Bar: 500 µm. (C) Photomicrograph of a fragment of humerus under polarized light, showing dark (white arrow), intermediate (arrowhead), and light (black arrow) osteons. Bar: 0.2 mm. (D) Photomicrograph of a physeal fracture fragment in the right femur under polarized light, showing the predominantly transversal organization of collagen fibres in bone trabeculae (arrows), with absence of osteons. Bar: 0.2 mm.

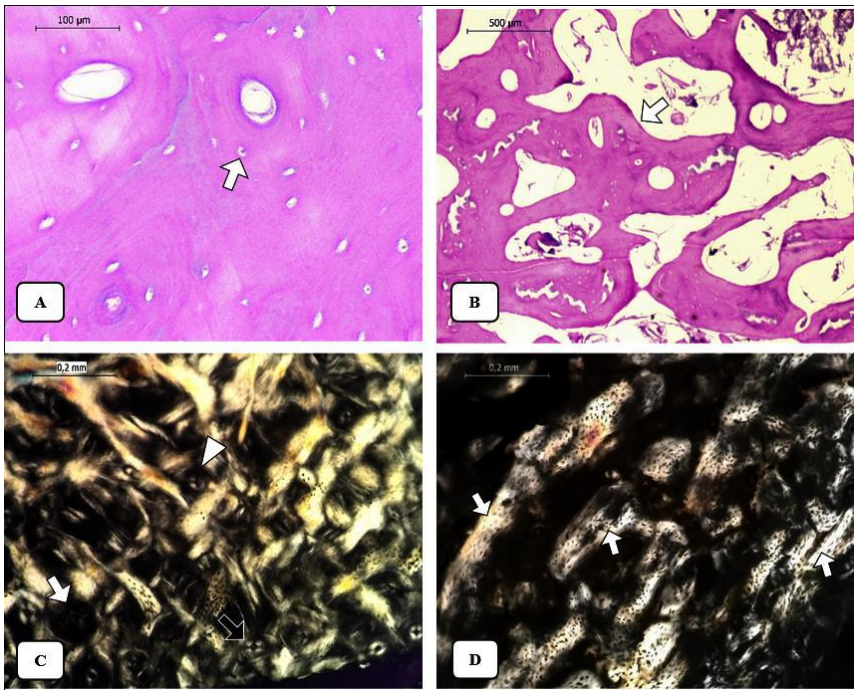

Source: The authors.

Figure 5. Scanning electron microscopy of the fracture surface of femur and humerus of *Cerdocyon thous* submitted to the three-point bending test. (A) Photomicrograph of a fragment of the cranial face of a fracture in the femur showing the arrangement of cortical bone tissue with the presence of osteons (arrow). Bar: 500 µm. (B) Magnification of A, showing osteons with slightly distinct interstitial lamellae and smooth surface, showing a deflection mechanism (arrow). Bar: 10 µm. (C) Photomicrograph of a fragment of the caudal fracture face in the humerus, where a large number of osteons (white arrow), Volkmann channels (black arrow), and microcracks (arrowhead) are observed. Bar: 500 µm. (D) Magnification of C, showing the longitudinal disposition of collagen fibres in the lamellae (arrow), and the aspect of delamination in the osteon. Bar: 10µm. (E) Photomicrograph of a fragment of a fracture in the proximal humerus epiphysis, showing the formation of bone trabeculae (arrow). Bar: 500 µm. (F) Physeal fracture surface of the right femur showing trabecular bone tissue, in which bone trabeculae with collagen fibres without apparent organization (arrow) and osteocyte gaps (arrowheads) are observed. Bar: 100 µm.

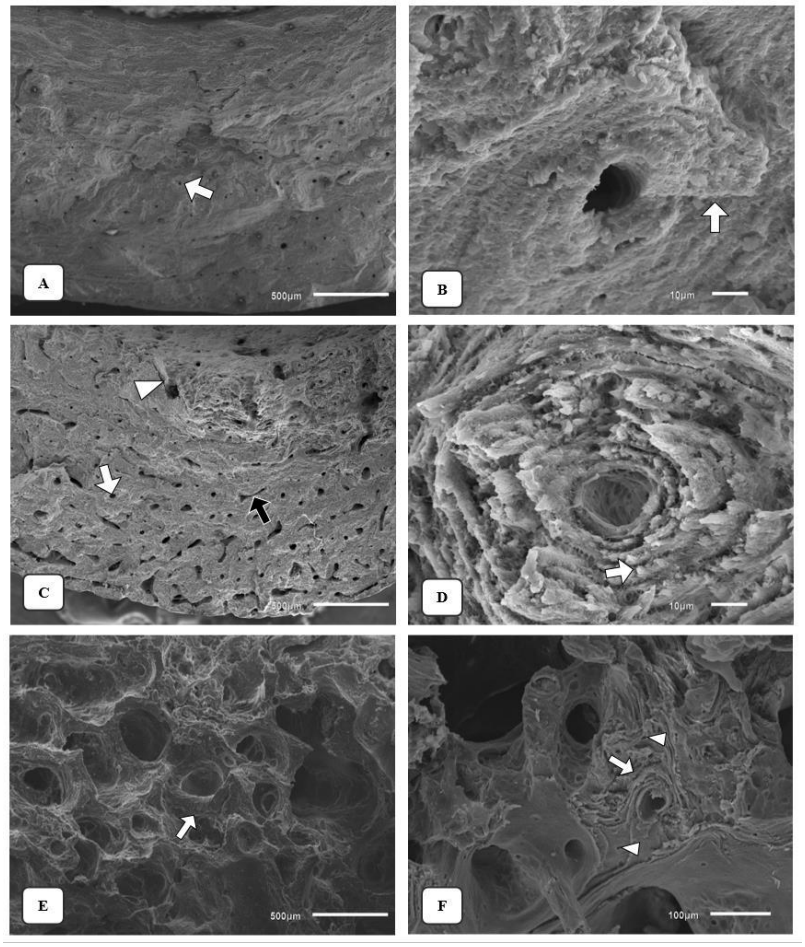

Source: The authors.

In the axial compression samples, there were differences between diaphyseal and physeal fractures. In diaphyseal samples, despite the irregular layout of the fracture line, the surface was smooth, with few evident microcracks, suggesting rupture by deflection. In physeal fractures, the patterns of rupture were diverse. There were regions made up of cartilaginous tissue from the physeal line, in addition to primary bone tissue, arranged in trabeculae, with collagen fibres without a standardized organization (Fig 5e and 5f).

The qualitative mineral distribution obtained from the femur and humerus samples (Figure 6a - 6f) demonstrated homogeneous distribution throughout the fracture surface for bones of both assays. Regarding the quantitative evaluation (Figure 6g), there was greater detection of calcium in the left femurs, when related to the left humerus (three-point bending test). For the

bones submitted to axial compression, there were differences only between the phosphorus values, with higher values in humerus. The proportion ratio between calcium and phosphorus established was: 1.55:1 for the left femurs; 1.73:1 for right femurs; 1.27:1 for left humerus; and 1.99:1 for right humerus. Simple linear regression analysis revealed no significant influence of the mineral content in the mechanical properties in all the samples tested.

Figure 6. Distribution of calcium and phosphorus (g/mol) on the bone surface of *Cerdocyon thous* femur and humerus. (A) Distribution of minerals present on the fracture surface in the left femur. O: oxygen; P: phosphorus; Ca: calcium; Mg: magnesium; K: potassium; Al: aluminium; F: fluorine. Bar: 300 µm. (B) Spatial distribution of calcium left femur surface. Bar: 300 µm. (C) Spatial distribution of phosphorus on the left femur surface. Bar: 300 µm. (D) Distribution of minerals present on the right femur surface. C: carbon; O: oxygen; P: phosphorus; Ca: calcium; Au: gold; Na: sodium; S: sulphur. Bar: 200 µm. (E) Spatial distribution of calcium on the right femur surface. Bar: 200 µm. (F) Spatial distribution of phosphorus on the right femur surface. Bar: 200 µm. (G) Graph of the quantitative distribution of calcium (Ca) and phosphorus (P) in the evaluated bones. LF: left femur; LH: left humerus; RF: right femur; RH: right humerus. * Statistically different means by the Tukey test (p <.05). ns: not significant.

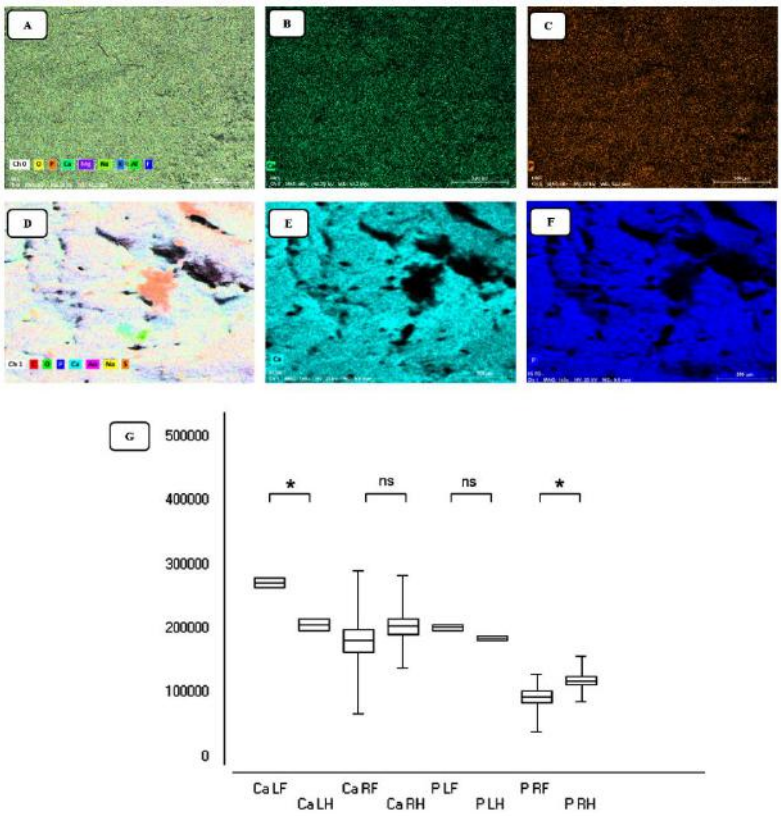

Source: The authors.

4. Discussion

The results of the experiment indicate that the femur and humerus have a ductile-fragile mechanical behaviour, with superiority of the humerus in terms of maximum load and strength, both in bending and compression loads. It was also observed that both properties exhibited higher values in compression tests, when compared to flexion. In the three-point bending test, the diaphysis circumference had a significant influence on the elastic modulus of both bones, while the maximum load supported by the humerus was related to bone length and weight. Under compression forces, the maximum load is influenced by humeral

diaphyseal circumference. Microscopically, there was a predominance of collagen fibres in an intermediate and longitudinal arrangement, with a deflection mechanism being noted on the cranial bone surfaces, while delamination was more evident on the caudal sides of bone fragments submitted to bending tests. In bones fractured under compression, the diaphyseal fragments had intermediate and longitudinal collagen fibres, while in physeal fragments, there were no evident collagen arrangement; all fracture surfaces indicate deflection as rupture mechanism. Furthermore, the mineral content of calcium was significantly higher in the left femur than in the left humerus, while right humerus contained more phosphorus than right femurs.

As regards the mechanical behaviour of the bones in both three-point bending and axial compression tests, it was observed that the femur and humerus have a ductile-fragile behaviour, with the strength and tenacity being greater in the humerus. Based on the results, it is possible to note the relationship between the values of maximum load and work by the bones until rupture, and it is possible to conclude that the humerus resists the greatest mechanical load until the time of fracture when compared to the femur, in addition to accumulating more energy until its rupture. Such differences can be related to the characteristic geometric conformation of the studied bones, since variations in size, mass, and cross-sectional area are known to influence bone mechanical properties (Bouxsein et al. 1999; Bouxsein and Karasik 2006; Lochmüller et al. 2002a, b, c; Müller et al. 2003).

It was observed in the present study that the femur supports a load of up to 450.68 ± 15.39 N until the occurrence of the fracture. When evaluating the mechanical behaviour of femurs of domestic dogs in the three-point flexion test, Saha et al. (1977) reported values of 1366 ± 253 N, considerably higher than those found for *Cerdocyon thous*. Notably, this discrepancy may be related to the size of the bones used by the authors, since domestic dogs have a high variation in the size and morphology of the femur due to racial particularities (Palierne et al. 2008).

From the results obtained for the linear regression, it is possible to observe that animals that have a longer, heavier, and wider humerus are more resistant to fractures caused by bending forces. In the femur, only the wider diaphysis is sufficient to make *C. thous* more resistant to fractures of the same cause.

In the femur under axial compression loads, complex fractures were the most prevalent, being this type the most serious, since several bone fragments are produced due to the dissipation of high impact load on the bone (Cordey 2000; Einhorn 1992; Turner and Bur 1993). Such results demonstrate that, when subjected to compression loads, the femur presents greater structural damage when compared to the humerus. This fact makes it possible to use different forms of therapeutic approach for compression fractures in each of these bones.

Most of the fractures observed in the three-point bending test were classified as simple, varying between the transverse (A3) and oblique (A2) types. These results corroborate those obtained by Loffredo and Ferreira (2007) who described the occurrence of oblique and transverse fractures in bovine tibiae fragments subjected to the three-point bending test, indicating that such morphological presentations are the most common in this type of test. However, we emphasise that such data cannot be fully compared, since the species and size of the fragments used by the author are different from those used in the present study. Simple transverse (A3) and oblique (A2) fractures originate from compression or flexion loads (Cordey 2000; Einhorn 1992; Turner and Bur 1993), while those of the fragmented wedge type (B3) result exclusively application of flexural loads (Müller et al. 2012). This statement was confirmed in the present study, since all fractures, whether type A or B, originated from the three-point bending test.

Based on the statistical results, there were no significant influence of the area occupied by transverse collagen fibres on bone mechanical properties in both assays. These findings agree with Holanda et al. (1999), who also did not find significant results for linear correlation between the area occupied by collagen fibres and the maximum load supported by rabbit femurs in the three-point bending test. The organization of collagen fibres inside the osteon is one of the most important factors in bone biomechanics. According to Heřt et al. (1994) and Martin and Boardman (1993), bone has greater resistance when the load

application occurs in the same direction as the orientation of the osteons in the cortical bone. The intermediate osteons have collagen fibres arranged in a longitudinal and transverse direction interspersed between the lamellae (Ascenzi and Bonucci 1968). Dark osteons, composed of longitudinal fibres, are commonly found in regions of the bone that support higher tensile loads, while transversal fibres are more prevalent in places subjected to compression (Martin and Boardman 1993).

In view of this information, it was expected that more clear osteons would be found in the fracture region of bones subjected to compression, since these fibres are arranged perpendicular to the axis of application of the compression load. However, there was a predominance of intermediate osteons, opposing the expected hypothesis. This allows us to consider that bone regions with the presence of fibres arranged in alternating directions may be more predisposed to the appearance of fractures caused by compression loads.

The spatial arrangement of collagen fibres observed here for *C. thous* bone samples has been reported in other mammalian species. Martin et al. (1996) confirmed that collagen fibres arranged in a longitudinal direction have greater resistance when compared to transversal fibres when evaluating equine cortical bone. Findings similar to the present study were also reported by Ramasamy and Akkus (2007) in the cortical bone of rats.

The large amount of longitudinal and intermediate fibres observed in the fractures generated under the three-point bending test is directly related to the fracture mechanism. As the load flexural in form, fractures occurred more easily when the load was applied perpendicular to the collagen fibres (Heřt et al 1994). Although there was no significant linear regression between the organization of collagen fibres and the mechanical properties obtained in the test, a greater number of intermediate osteons was observed in the humerus, which showed greater maximum strength when compared to the femurs. Such information may suggest that the organisation of collagen fibres solely does not act as a determining factor for bone strength. Other unassessed variables, such as the diameter and density of osteons per area (Moyle et al. 1978) may have a significant influence on the mechanical properties of the *Cerdocyon thous* bone, requiring further evaluation.

Based on the fracture surface morphology assessed by SEM, it was possible to observe rupture by deflection on the cranial bone face and delamination on the caudal face of bones fractured by bending loads. It is known that the deflection mechanism, which was also observed on fractures caused by axial compression, occurs through the transversal break of the osteon at a specific point, giving the structure a step aspect, with a surface that appears smooth (Hastings and Ducheyne 1984). This may be caused by the unstable propagation of the microcrack through the bone cementation line, in addition to the reduced rupture energy (Currey 2012; Vashishth 2004). In turn, the mechanism of delamination observed on the caudal faces of the fracture surface of both bones occurs by the rupture of the lamellae in different stages, giving the osteon a pull-out aspect, with groups of mineralized collagen fibres and the appearance of splinters. The fracture surface, in this case, becomes rough (Hastings and Ducheyne 1984), and may originate as a result of the transition between the ductility and fragility properties of the specimen, as the rougher area indicates the location of greater energy absorption before fracture occurs (Currey 2012; Loffredo and Ferreira 2007).

The microcracks present on the fracture surface, such as those observed here, occur due to the redistribution of stresses in the bone structure. Another factor that promotes the appearance of these microcracks is the normal conformation of the bone containing structures that initiate the nucleation of cracks easily and propagate them with greater intensity, such as cementation lines (Fleck and Eifler 2003; Koester et al. 2008; Nalla et al. 2005; Vashishth et al. 1997; Zimmermann et al. 2009), since their content is predominantly mineral (Skedros et al. 2005). However, the spread of microcracks is prevented by other structures that assist in the redistribution of stresses, such as osteonal lamellae (Loffredo and Ferreira 2007).

Considering the bone mineral content, a significant difference was observed in the calcium content between the evaluated bones, in which the left femur presented a higher concentration of the mineral. Meanwhile, right humerus present a considerable higher value of phosphorus. Interestingly, there were no statistically significant influence of the mineral

concentration on the mechanical properties obtained in both three-point bending and axial compression tests. It was expected that the greater detection of calcium through the EDS could explain the lower maximum load supported by the left femur, since the greater the degree of bone mineralisation, the lower the capacity of collagen fibres to undergo deformation, resulting in increased hardness and reduced bone strength (Martin and Boardman 1993). This fact is corroborated by Wang and Feng (2005), who, when evaluating the effects of demineralisation and calcination on the mechanical properties of the bovine femoral cortical bone, observed a reduction in the modulus of elasticity, emphasising the importance of the presence of mineralized bone matrix on the mobility of type I collagen fibres. This statement is also corroborated by Hoc et al. (2006), since, when studying the influence of osteonal mineralization on the elasticity module of bovine cortical bones, they found a high correlation value for the variables, with 75% of the variations in the modulus of elasticity were explained by changes in the mineral content. With this, Currey (1990) states that an increase in mineralization makes the bone more fragile by reducing energy absorption, and consequently, there is less elastic deformation. The data observed here show a greater detection of calcium in the left femur, which also presented a greater modulus of elasticity. A high modulus of elasticity indicates greater resistance to the appearance of elastic deformation, and therefore greater toughness. When evaluating the mechanical behaviour of long bones of domestic dogs in flexion tests at three and four points, Borders et al. (1977) observed a high influence of mineral content on the fracture moment ($r = 0.901$) and modulus of elasticity ($r = 0.887$), differing from the results observed here.

In this study, the proportion ratio between calcium and phosphorus established was: 1.55:1 for the left femurs; 1.73:1 for right femurs; 1.27:1 for left humerus; and 1.99:1 for right humerus. When determining the mineral content in the femur and tibia of greyhound dogs, Bloebaum et al. (1997) found Ca:P ratio values ranging from 1.62:1 to 1.65:1—values higher than those found in the present study. Our results also differ from those measured by Loffredo and Ferreira (2007), who found values of 1.7:1 in bovine cortical bone. They also disagree with Miculescu et al. (2012), who, when researching the mineral profile of bone fragments from human femurs, found the Ca:P ratio with a value of 1.69:1. The results found here indicate a reduction in the concentration of calcium in relation to the content of phosphorus. However, we emphasise on the importance of developing new studies aimed at tracing the bone mineral profile of the *Cerdocyon thous* using a larger sample size, which could help compare the relationship between the mineral content and bone mechanical properties of the species in question.

We expect that the information provided by the present study will shed light on the pathophysiological mechanism of fractures caused by flexion forces in the long bones of *Cerdocyon thous*. With this understanding, the choice of therapeutic methods for such injuries is facilitated, which directly contributes to the rehabilitation and preservation of the species.

5. Conclusion

There are significant differences in the mechanical behaviour of the femur and humerus of *Cerdocyon thous*. Humerus are more resistant than femurs in both bending and compression loads. Longer, heavier, and wider humerus are more resistant to fractures caused by flexion forces, while in the femur, only the widest diaphysis is sufficient to make it more resistant to ruptures of the same cause. In the humerus submitted to the compression test, the maximum load is proportional to the width of the bone diaphysis. Both bones exhibit the same microscopic pattern in diaphyseal fractures, which did not interfere significantly with their mechanical properties. These results enable the prediction of the mechanical behaviour of the femur and humerus of *Cerdocyon thous* against trauma caused by flexion and compression impacts, thus leading to more effective therapeutic measures in such situations.

Acknowledgments

The authors acknowledge the Cell Ultrastructure Laboratory Carlos Alberto Redins (LUCCAR) of the Universidade Federal do Espírito Santo and to the notice MCT/FINEP/CT-INFRA - PROINFRA 01/2006 for the analysis of scanning electron microscopy.

This work was supported by the Fundação de Amparo à Pesquisa e Inovação do Espírito Santo (FAPES) (116/2017 – 8060422). This study was financed in part by the Coordenação de Aperfeiçoamento de Pessoal de Nível Superior - Brasil (CAPES) - Finance Code 001.

References

ABNT, Associação Brasileira de Normas Técnicas. (2017) *NBR 7190 - Projeto de estruturas de madeira*. Rio de Janeiro, 1997. <https://www.abntcatalogo.com.br/norma.aspx?ID=3395>. Access 04 jun. 2021, 20:36.

Araujo Cezar, H. R.; Abrantes, S. H. F.; de Lima, J. P. R.; de Medeiros, J. B.; Abrantes, M. M. R.; da Nóbrega Carreiro, A. & de Lucena Barbosa, J. P. (2021). Mamíferos silvestres atropelados em estradas da Paraíba, Nordeste do Brasil. *Brazilian Journal of Development*, 7(3), 30694-30698. https://doi.org/10.34117/bjdv7n3-679

Ascenzi, A. & Bonucci, E. (1968). The compressive properties of single osteons. *The Anatomical Record*, 161(3):377-391. https://doi.org/10.1002/ar.1091610309

ASTM, American Society for Testing and Materials. (2017). *Standard test methods for flexural properties of unreinforced and reinforced plastics and electrical insulating materials*. ASTM D790-17. <https://www.astm.org/d0790-03.html>. Access 12 sep 2020, 09:18.
Berta, A. (1982). *Cerdocyon thous*. *Mammalian Species*, 186, 1-4. https://doi.org/10.2307/3503974

Bloebaum, R. D.; Skedros, J. G.; Vajda, E. G.; Bachus, K. N.; Constantz, B. R. (1997). Determining mineral content variations in bone using backscattered electron imaging. *Bone*, 20(5), 485-490. https://doi.org/10.1016/S8756-3282(97)00015-X

Borders, S.; Petersn, K. R. & Orne, D. (1977). Prediction of bending strength of long bones from measurements of bending stiffness and bone mineral content. *Journal of Biomechanical Engineering*, 99(1), 40-44. https://doi.org/10.1115/1.3426267

Bouxsein, M. L.; Coan, B. S. & Lee, S. C. (1999). Prediction of the strength of the elderly proximal femur by bone mineral density and quantitative ultrasound measurements of the heel and tibia. *Bone*, 25(1), 49-54. https://doi.org/10.1016/S8756-3282(99)00093-9

Bouxsein, M. L. & Karasik, D. (2006). Bone geometry and skeletal fragility current osteoporosis reports. *Current Osteoporosis Reports*, 4(2), 49-56. https://doi.org/10.1007/s11914-006-0002-9

Brum, T. R.; Santos-Filho, M.; Canale, G. R. & Ignácio, A. R. A. (2018). Effects of roads on the vertebrates diversity of the Indigenous territory Paresi and its surrounding. *Brazilian Journal of Biology*, 78(1), 125-132. https://doi.org/10.1590/1519-6984.08116

Carlton, W. W. & Mcgavin, M. D. (1998). *Patologia Veterinária Especial de Thonson*, 2nd edn. Artes Médicas Sul, Porto Alegre.

Castilho, M. S.; Rahal, S. C.; Mamprim, M. J.; Inamassu, L. R.; Melchert, A.; Agostinho, F. S.; Mesquita, L. R.; Teixeira, H.F.; & Teixeira, C. R. (2018). Radiographic measurements of the hindlimbs in crab-eating foxes (*Cerdocyon thous*, Linnaeus, 1766). *Anatomia, Histologia, Embryologia*, 47(3), 216-221. https://doi.org/10.1111/ahe.12344

Cordey, J. (2000). Introduction: Basic concept and definitions in mechanics. *Injury*, 31, 1-84. https://doi.org/10.1016/S0020-1383(00)80039-X

Courtenay, O. & Maffei, L. (2004). *Cerdocyon thous* (Linnaeus, 1766). *Canid Action Plan*. IUCN Publications, Gland, Switzerland.

Currey, J. D. (1990). Physical characteristics affecting the tensile failure properties of compact bone. *Journal of Biomechanics*, 23(8), 837-844. https://doi.org/10.1016/0021-9290(90)90030-7

Currey, J. D. (1970). The mechanical properties of bone. *Clinical Orthopaedics and Related Research*, 73, 210-231. https://doi.org/10.1097/00003086-197011000-00023

Currey, J. D. (2012). The structure and mechanics of bone. *Journal of Material Sciences*, 47(1), 41-54. https://doi.org/10.1007/s10853-011-5914-9

Einhorn, T. (1992). Bone strength: the bottom line. *Calcified Tissue International*, 51(5), 333-339. https://doi.org/10.1007/BF00316875

Fleck, C. & Eifler, D. (2003). Deformation behaviour and damage accumulation of cortical bone specimens from the equine tibia under cyclic loading. *Journal of Biomechanics*, 36(2), 179-189. https://doi.org/10.1016/S0021-9290(02)00364-0

Ginsberg, J.R.; & Macdonald, D.W. (1990). *Foxes, wolves, jackals, and dogs: an action plan for the conservation of canids*. IUCN Publications, Gland, Switzerland.

Grilo, C. et al. (2018). Brazil road-kill: a data set of wildlife terrestrial vertebrate road-kills. *Ecology*, 99(11), 2625.

Hastings, G. W. & Ducheyne, P. (1984). *Natural and living biomaterials*. CRC Press, Boca Raton.

Heřt, J.; Fiala, P.; & Petrtýl, M .(1994). Osteon orientation of the diaphysis of the long bones in man. *Bone*, 15(3), 269-277. https://doi.org/10.1016/8756-3282(94)90288-7

Hoc, T.; Henry, L.; Verdier, M.; Aubry, D. Sedel, L. & Meunier, A. (2006). Effect of microstructure on the mechanical properties of Haversian cortical bone. *Bone*, 38(4), 466-474. https://doi.org/10.1016/j.bone.2005.09.017

Holanda, A; Volpon, J. B. & Shimano, A. C. (1999). Efeitos da orientação das fibras de colágeno nas propriedades mecânicas de flexão e impacto dos ossos. *Revista Brasileira de Ortopedia*, 34(11/12), 579-584.

Koester, K. J.; Ager, J. W. & Ritchie, R. O. (2008). The true toughness of human cortical bone measured with realistically short cracks. *Nature Materials*, 7(8), 672-677. https://doi.org/10.1038/nmat2221

Lochmüller, E. M.; Bürklein, D.; Kuhn, V.; Glaser, C.; Müller, R.; Glüer, C. C. & Eckstein, F. (2002a). Mechanical strength of the thoracolumbar spine in the elderly: prediction from in situ dual-energy X-ray absorptiometry, quantitative computed tomography (QCT), upper and lower limb peripheral QCT, and quantitative ultrasound. *Bone*, 31(1), 77-84. https://doi.org/10.1016/S8756-3282(02)00792-5

Lochmüller, E. M.; Groll, O.; Kuhn, V. & Eckstein, F. (2002b). Mechanical strength of the proximal femur as predicted from geometric and densitometric bone properties at the lower limb versus the distal radius. *Bone*, 30(1), 207-216. https://doi.org/10.1016/S8756-3282(01)00621-4

Lochmüller, E. M.; Lill, C. A.; Kuhn, V.; Schneider, E. & Eckstein, F. (2002c). Radius bone strength in bending, compression, and falling and its correlation with clinical densitometry at multiple sites. *Journal of Bone and Mineral Research*, 17(9), 1629-1638. https://doi.org/10.1359/jbmr.2002.17.9.1629

Loffredo, M. D. C. M. & Ferreira, I. (2007). Resistência mecânica e tenacidade à fratura do osso cortical bovino. *Research on Biomedical Engineering*, 23(2), 159-168.

Markel, M. D.; Sielman, E.; Rapoff, A. J. & Kohles, S. S. (1994). Mechanical properties of long bones in dogs. *American Journal of Veterinary Research*, 55(8), 1178-1183

Martin, R. B. & Boardman, D. L. (1993). The effects of collagen fiber orientation, porosity, density, and mineralization on bovine cortical bone bending properties. *Journal of Biomechanics*, 26(9); 1047-1054. https://doi.org/10.1016/S0021-9290(05)80004-1

Martin, R. B.; Lau, S. T.; Mathews, P. V.; Gibson, V. A. & Stover, S. M. (1996). Collagen fiber organization is related to mechanical properties and remodeling in equine bone. A comparsion of two methods. *Journal of Biomechanics*, 29(12), 1515-1521. https://doi.org/10.1016/S0021-9290(96)80002-9.

Martins, F. P.; Souza, E. C.; Bernardes, F. C. S.; Abidu-Figueiredo, M.; Kasper, C. B. & Souza-Junior, P. (2021). Anatomical variations in cervical vertebrae in two species of neotropical canids: What is the meaning? *Anatomia, Histologia, Embryologya*, 50(1), 212-217. https://doi.org/10.1111/ahe.12609

Miculescu, F.; Stan, G. E.; Ciocan, L. T.; Miculescu, M.; Berbecaru, A. & Antoniac, I. (2012). Cortical bone as resource for producing biomimetic materials for clinical use. *Digest Journnal of Nanomater Biostructures*, 7(4), 1667-1677.

Morse, A. (1945). Formic acid-sodium citrate decalcification and butyl alcohol dehydration of teeth and bones for sectioning in paraffin. *Journal of Dental Research*, 24(3-4), 143-153. https://doi.org/10.1177/00220345450240030501

Moyle, D. D.; Welborn III, J. W. & Cooke, F. W. (1978). Work to fracture of canine femoral bone. *Journal of Biomechanics*, 11(10-12), 435-440. https://doi.org/10.1016/0021-9290(78)90055-6

Müller, M. E.; Webber, C. E. & Bouxsein, M. L. (2003). Predicting the failure load of the distal radius. *Osteoporosis International*, 14(4), 345-352. https://doi.org/10.1007/s00198-003-1380-9

Nalla, R. K.; Stölken, J. S.; Kinney, J. H. & Ritchie, R. O. (2005). Fracture in human cortical bone: local fracture criteria and toughening mechanisms. *Journal of Biomechanichs*, 38(7), 1517-1525. https://doi.org/10.1016/j.jbiomech.2004.07.010

Nishioka, R. S.; Yamasaki, M. C.; De Melo Nishioka, G. N. & Balducci, I. (2010). Estudo da ocorrência de micro deformações ao redor de três implantes de hexágono externo, sob a influência da fundição de coifas plásticas e usinadas. *Brazilian Dental Journal*, 13(3/4), 15-21. https://doi.org/10.14295/bds.2010.v13i3/4.63

Ossa-Nadjar, O. & Ossa, J. (2013). Fauna silvestre atropellada en dos vías principales que rodean los Montes de María, Sucre, Colombia. *Revista Colombiana Ciencia Animal*, 5, 158-164. https://doi.org/10.24188/recia.v5.n1.2013.481

Palierne, S.; Mathon, D.; Asimus, E.; Concordet, D.; Meynaud-Collard, P.; Autefage, A. (2008). Segmentation of the canine population in different femoral morphological groups. Research in Veterinary Science, 85, 407-417. https://doi.org/10.1016/j.rvsc.2008.02.010

Pessutti, C.; Santiago, M. E. B. & Oliveira, L. T. F. (2001). Order Carnivora, Family Canidae (Dogs, Foxes, Maned foxes). In: Fowler, M. E. & Cubas, Z. S. (eds.) *Biology, medicine, and surgery of South American wild animals*, Iowa State University Press.

Pinheiro, L. L.; Branco, É.; Souza, D. C.; Pereira, L. H. C. & Lima, A. R. (2014). Description of plexus brachial of crab-eating foxes (*Cerdocyon thous* Linnaeus, 1766). *Ciência Animal Brasileira*, 15, 213-219. https://doi.org/10.1590/1809-6891v15i220309

Ramasamy, J. G. & Akkus, O. (2007). Local variations in the micromechanical properties of mouse femur: the involvement of collagen fiber orientation and mineralization. *Journal of Biomechanichs*, 40(4), 910-918. https://doi.org/10.1016/j.jbiomech.2006.03.002

Rho, J. Y.; Kuhn-Spearing, L. & Zioupos, P. (1998). Mechanical properties and the hierarchical structure of bone. *Medical Engineering & Physics*, 20, 92-102. https://doi.org/10.1016/S1350-4533(98)00007-1

Saha, S.; Martin, D. L. & Phillips, A. (1977). Elastic and strength properties of canine long bones. *Medical & Biological Engineering & Computing*, 15(1), 72-74. https://doi.org/10.1007/BF02441578

Salter, R. B. & Harris, W. R. (1963). Injuries Involving the Epiphyseal Plate. *Journal of Bone and Joint Surgery*, 45(3), 587–622.

Skedros, J. G.; Holmes, J. L.; Vajda, E. G. & Bloebaum, R. D. (2005). Cement lines of secondary osteons in human bone are not mineral-deficient: New data in a historical perspective. Anatomical Record, 286(1), 781-803. https://doi.org/10.1002/ar.a.20214

Trapp, S. M.; Iacuzio, A. I.; Barca Junior, F. A.; Kemper, B.; Silva, L. C. da; Okano, W.; Tanaka, N. M.; Grecco, F. C. de A. R.; Cunha Filho, L. F. C. da; Sterza, F. A. M. (2010). Causas de óbito e razões para eutanásia em uma população hospitalar de cães e gatos. Brazilian Journal of Veterinary Research and Animal Science, 47(5), 395-402. https://doi.org/10.11606/issn.1678-4456.bjvras.2010.26821

Turner, C. H. & Burr, D. B. (1993). Basic biomechanical measurements of bone: a tutorial. *Bone* 14(4), 595-608. https://doi.org/10.1016/8756-3282(93)90081-K

Unger, M.; Montavon, P. M. & Heim, U. F. A. (1990). Classification of fractures of long bones in the dog and cat: introduction and clinical application. *Veterinary and Comparative Orthopaedics and Traumatology*, 3, 41-50. https://doi.org/10.1055/s-0038-1633228

Vashishth, D.; Behiri, J. C. & Bonfield, W. (1997). Crack growth resistance in cortical bone: concept of microcrack toughening. *Journal of Biomechanics*, 30(8), 763-769. https://doi.org/10.1016/S0021-9290(97)00029-8

Vashishth, D. (2004). Rising crack-growth-resistance behavior in cortical bone: implications for toughness measurements. *Journal of Biomechics*, 37(6), 943-946. https://doi.org/10.1016/j.jbiomech.2003.11.003

Vélez, J.; Ramírez, J. & Aristizábal, O. (2018). An anatomic description of intrinsic brachial muscles in the crab-eating fox (*Cerdocyon thous*, Linnaeus 1776) and report of a variant arterial distribution. *Anatomia, Histologia, Embryolgia*, 47(2), 180-183. https://doi.org/10.1111/ahe.12330

Wang, T. & Feng, Z. (2005). Dynamic mechanical properties of cortical bone: The effect of mineral content. *Materials Letters*, 59(18), 2277-2280. https://doi.org/10.1016/j.matlet.2004.08.048

Wang, X.; Shen, X.; Li, X. & Agrawal, C. M (2002). Age-related changes in the collagen network and toughness of bone. *Bone* 31, 1-7. https://doi.org/10.1016/S8756-3282(01)00697-4

Zadpoor, A. A. (2015). Mechanics of biological tissues and biomaterials: current trends. *Materials*, 8(7), 4505-4511. https://doi.org/10.3390/ma8074505

Zimmermann, E. A.; Launey, M. E.; Barth, H. D. & Ritchie, R. O. (2009). Mixed-mode fracture of human cortical bone. *Biomaterials* 30(29), 5877-5884. https://doi.org/10.1016/j.biomaterials.2009.06.017.